ROG.e 2024
ISSN 2525-7579
biblioteca.ibp.org.br

Technical Paper

Promoted and Organized by:

Modelo de super resolução para melhorar a qualidade de imagens de arenito utilizando transfer learning

Super resolution model to improve sandstone image quality using transfer learning

Vinícius Rabello Rodrigues , Paulo André de Mesquita e Bomfim Leite de Castro , Yasamin Fazeli , Reza Arefidamghani , Hamidreza Anbarlooei.

Abstract:

Obtaining high-quality underground images is crucial for optimizing resource extraction in the oil and gas industry, yet it remains challenging due to financial and technical constraints. Deep learning methods offer a promising solution to this challenge, particularly through super-resolution techniques, which enhance image quality. In this study, we investigate the efficacy of synthetic data generation coupled with transfer learning in addressing the need for extensive real data collection. By pre-training a model with synthetic data and fine-tuning it with a smaller set of authentic sandstone images, significant improvements in model performance were observed. Evaluation metrics, including Structural Similarity Index Method (SSIM) and Mean Squared Error (MSE), consistently demonstrated the superiority of Transfer Learning-Super-Resolution Convolutional Neural Network (TL-SRCNN) over standard SRCNN, even with reduced datasets. While the initial synthetic data generation process utilized spheres with uniform properties, future advancements incorporating diverse grain types hold promise for further enhancing model realism and efficacy. Our findings suggest that the integration of synthetic data generation with transfer learning presents a viable solution for overcoming the challenges associated with real data acquisition in underground imaging applications, offering cost-effective and efficient alternatives to traditional imaging approaches.

Keywords: super resolution; SRCNN; convolutional neural networks; sandstone; transfer learning

A obtenção de imagens subterrâneas de alta qualidade é crucial para otimizar a extração de recursos na indústria de petróleo e gás, mas permanece desafiadora devido a restrições financeiras e técnicas. Métodos de aprendizado profundo oferecem uma solução promissora para esse desafio, especialmente através de técnicas de super-resolução, que melhoram a qualidade da imagem. Neste estudo, investigamos a eficácia da geração de dados sintéticos combinada com aprendizado de transferência para lidar com a necessidade de extensa coleta de dados reais. Ao pré-treinar um modelo com dados sintéticos e ajustá-lo com um conjunto menor de imagens autênticas de arenito, observamos melhorias significativas no desempenho do modelo. Métricas de avaliação, incluindo o Índice de Similaridade Estrutural (SSIM) e o Erro Quadrático Médio (MSE), consistentemente demonstraram a superioridade da Rede Neural Convolucional de Super-Resolução com Aprendizado de Transferência (TL-SRCNN) sobre SRCNN padrão, mesmo com conjuntos de dados reduzidos. Embora o processo inicial de geração de dados sintéticos tenha utilizado esferas com propriedades uniformes, futuros avanços incorporando diversos tipos de grãos prometem melhorar ainda mais a realidade e eficácia do modelo. Nossas descobertas sugerem que a integração da geração de dados sintéticos com aprendizado de transferência apresenta uma solução viável para superar os desafios associados à aquisição de dados reais em aplicações de imagem subterrânea, oferecendo alternativas eficientes e econômicas às abordagens de imagem tradicionais.

Palavras-chave: super resolution; SRCNN; redes neurais convolucionais; arenito; transfer learning.

Received: September 8th, 2024 | **Accepted:** July 7th, 2024 | **Available online:** September 23th, 2024
Article nº: 3319
DOI: https://doi.org/10.48072/2525-7579.roge.2024.3319

1. Universidade Federal do Rio de Janeiro - Instituto de Matemática Aplicada. Matemática Aplicada. BRASIL. E-mail: viniciusrabello@matematica.ufrj.br. (https://orcid.org/0009-0002-0968-5213). 2. Universidade Federal do Rio de Janeiro - Instituto de Matemática Aplicada. Matemática Aplicada. BRASIL. E-mail: paulo.andre@matematica.ufrj.br. (https://orcid.org/0009-0001-5147-8085). 3. K.N.Toosi University of Technology. Mathematics. IRAN. E-mail: yasfazelii@gmail.com. (https://orcid.org/0009-0007-1875-4598). 4. Universidade Federal do Rio de Janeiro - Instituto de Matemática Aplicada. Institute of Mathematics - UFRJ. BRASIL. E-mail: reza.arefi@matematica.ufrj.br. (https://orcid.org/0000-0001-9885-2532). 5. Universidade Federal do Rio de Janeiro - Instituto de Matemática Aplicada. matematica aplicada. BRASIL. E-mail: hamid@matematica.ufrj.br. (https://orcid.org/0000-0002-3220-7255).

1 Introduction

In the oil and gas industry, obtaining and analyzing high-quality underground images is paramount for optimizing the extraction of resources. However, the acquisition of such images often proves to be financially and technically challenging due to limitations in instrument precision or computational capabilities. Similarly, the issue of balancing image resolution and X-ray exposure in computed tomography (CT) mirrors the challenges faced in the oil and gas industry. The resolution of CT images is usually limited by scanning devices and cost. The trade-off between higher resolution images and the associated complexities, costs, and exposure levels highlights the need for cost-effective and efficient alternatives. To address this challenge and achieve enhanced image quality, advanced deep learning methods have emerged as a promising solution. In this context, leveraging super-resolution techniques offers a viable solution to enhance image quality while mitigating the drawbacks of traditional imaging approaches (see for example [Park, Park and Kang (2003)] and [Yang and Jiabao (2021)]). In this context, the term ”super-resolution” denotes the process of generating a high-resolution (HR) image from a low-resolution (LR) image.

In recent years, numerous studies have been conducted to enhance the resolution of digital rock images, e.g., sandstone and carbonate. For this purpose, deep learning techniques have been used, which are also being applied aggressively in many other engineering and science applications, to name few [Ahuja, Gupta, Rapole, Saxena, Hofmann, Day-Stirrat, Prakash and Yalavarthy (2022), Karimpouli, Kadyrov, Siegert and Saenger (2023), Da Wang, Shabaninejad, Armstrong and Mostaghimi (2021), Zhao, Saxena, Hofmann, Pradhan and Hows (2023)]. Wang et al. [Wang, Teng, He, Feng and Zhang (2019)], employed a 3D convolutional neural network to enhance the resolution of CT images of rock samples. Cai et al. [Cai,Yang, Meng, Qiu, Lei, and Xu (2024)], introduced a super resolution generative adversarial network approach for enhancing resolution and deblurring porous media μ-CT images [Cai et al. (2024)]. In another work Luo et al. [Luo, Sun, Zhang, Chi and Cui (2024)], proposed a multi-condition denoising diffusion probabilistic model for controlling the reconstruction of 3D digital rocks. Additionally, Soltanmohammadi and Faroughi [Soltanmohammadi and Faroughi (2023)] conducted a comparative analysis of super-resolution techniques for enhancing micro-CT images of carbonate rocks. In this study, we employ a model based on the well-established deep convolutional neural network architecture designed for super resolution. The SRCNN, which stands for Super-

Resolution Convolutional Neural Network [Dong, Loy, He and Tang (2015)], represents an advanced technique in the field of single image super-resolution (SR). It operates as a deep learning technique, designed to directly learn a seamless mapping from low-resolution to high-resolution images. This mapping is embedded within a deep convolutional neural network (CNN), serving as an advanced computational framework. Essentially, SRCNN takes a low-resolution image as input and employs intricate neural network layers to generate a corresponding high-resolution output. This model excels in enhancing image resolution, offering a promising solution for various applications requiring detailed image reconstruction. Overall, the utilization of advanced deep learning techniques and super-resolution methods presents an opportunity to overcome the limitations posed by conventional imaging processes, thereby facilitating more effective and economical resource extraction practices in the oil and gas sector.

However, the success of these models still relies on access to a sufficiently large dataset of low and high resolution training images, yet, this process is constrained mentioned before. In the present study, we introduced synthetic data generation alongside transfer learning as a promising strategy for addressing the these obstacles. Through the utilization of synthetic data for initial model pre-training and subsequent fine-tuning with a smaller set of authentic tomography images, notable enhancements has been observed in model performance while circumventing the necessity for large datasets.

2 Model

This section provides a detailed description of the algorithmic design, with a specific focus on the SRCNN architecture. Additionally, it introduces the dataset utilized for training, which comprises high-resolution images of sandstone slices. Subsequently, it delves into the evaluation metrics employed to examine and compar the performance of various super-resolution approaches.

2.1 SRCNN architecture

SRCNN, short for Super-Resolution Convolutional Neural Network, represents a machine learning approach in the realm of single image super-resolution (SR) [Dong et al. (2015)]. It has been designed to learn a seamless mapping from low-resolution to high-resolution images. This mapping is encapsulated within a deep convolutional neural network (CNN) layers. SRCNN has a relatively simple architecture compared to some other models [Ledig, Theis, Huszar, Caballero, Cunningham, Acosta, Aitken, Tejani, Totz, Wang and Shi(2017), Lim, Son, Kim, Nah and Lee

(2017), Zhang, Li, Li, Wang, Zhong and Fu (2018)], being easier to implement and understand. As consequence of this relative simplicity, it does not have the need for complicated pre and post processing tasks, can generate fast outputs and most importantly has lower demand for computational resources compared to other methods. Despite these advantages, the SRCNN has demonstrated competitive performance compared to more complex architectures [Soltanmohammadi et al. (2023)]. The SRCNN model consists of only three layers as shown in Figure 1. The first layer in the SRCNN model is responsible for extracting patches from the input image and representing them. It employs a convolutional layer with 64 filters, each with a kernel size of (9,9). The second layer, nonlinear functions are applied to map the low-resolution representations obtained from the previous layer to their corresponding high-resolution versions. This layer employs another convolutional layer with 32 filters and a kernel size of (1,1). Finally, in the third and last stage, the enhanced feature maps from the previous layer undergo further processing and refinement to reconstruct the high-resolution image. This stage involves a convolutional layer with 3 filters and a kernel size of (5,5). Following the completion of the first and second layers, the Rectified Linear Unit (ReLU) activation function is applied. This function is responsible for introducing nonlinearity into the network computations, essentially helping the model learn complex patterns and relationships within the data.

Figure 1-SRCNN architecture.

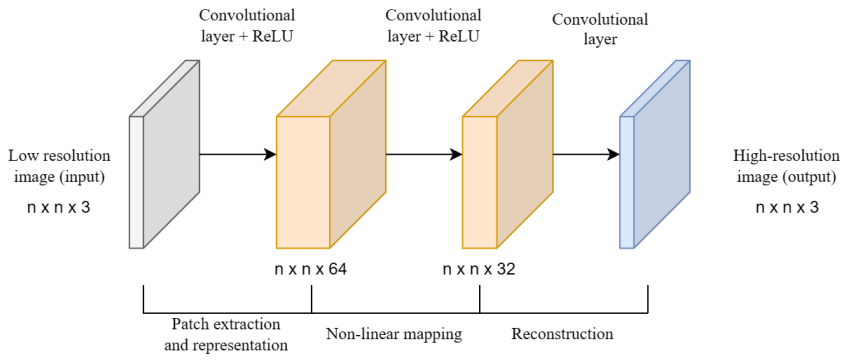

Source: Made by the authors.

2.2 Dataset

In the present work, the Super Resolution Dataset of Digital Rocks (DRSRD1-2D) produced by Wang, Armstrong, et al. [Wang, Mostaghimi and Armstrong (2019)], has been used for the training, validation and testing of our implementation of the SRCNN model. This library has a collection of 1000 high-resolution images extracted from slices of Bentheimer sandstone. Each image in this dataset is originally sized at 800x800 pixels. To simulate the specific scenario of the

present work, we have downsampled these images by a factor of 8x, to generate low-quality images. Subsequently, the SRCNN mod trained to recover the high-resolution images from these downsampled ones (see Figure 2). To facilitate the training, testing, and validation of our model, we partitioned the LR images and their HR counterparts into separate sets. This division ensures that our model can learn from a diverse range of examples during training, validate its performance on unseen data during validation, and assess its generalization ability on independent data during testing.

Figure 2- Dataset sample (left) and its low resolution version (right)

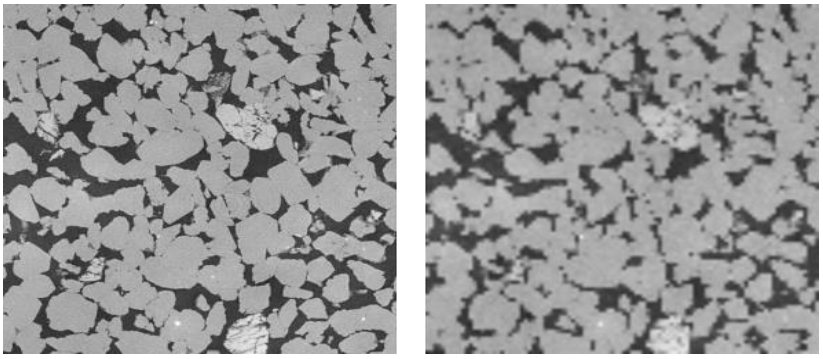

Source: Made by the authors.

3 Training

This section describes the training strategy implemented for our super-resolution model. The model has initially been trained exclusively on the DRSRD1-2D dataset. To overcome the scarcity of images in this dataset (or practical limitations), synthetic data were then generated. Subsequently, the model was trained on this augmented dataset. Following this, transfer learning was employed, refining the trained model further using images from the DRSRD1-2D dataset.

3.1 Training on DRSRD1-2D dataset

Initially, our training focused on the SRCNN model utilizing images solely from the DRSRD1-2D dataset. Table 1 presents a comparison between low-resolution (LR) and high-resolution (HR) images alongside the outputs produced by our model. Additionally, Figure 3 visually depicts this comparison. Despite the discernible enhancement our model offers to the quality of low-resolution sandstone im- ages, it encounters two main obstacles in practical applications: insufficient data for robust training and the considerable high cost of acquiring more data. To address this challenge, a viable solution emerges; we propose creating synthetic tomography images to complement the real data. This combined approach can help overcome data limitations and enhance our model performance in practical applications.

Figure 3- Low-resolution image (left), model response (middle), high-resolution image (right)

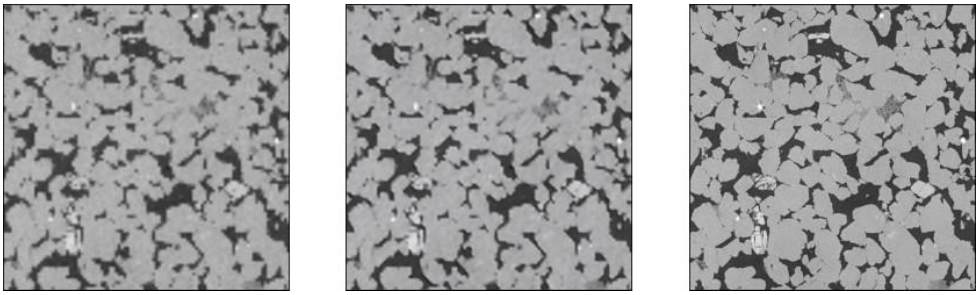

Source: Made by the authors.

Table 1- Comparative analysis of LR image and Model response against HR image

	SSIM	MSE
LR image vs. HR image	0.4845	0.0074
Model response vs. HR image	0.5021	0.0070

3.2 Synthesizing new data

The concept of generating synthetic porous rocks has been previously investigated, for example see [Blöcher and Zimmermann (2008)]. Within this context, we elaborate on our simplified adaptation of this concept. The sandstone grains have been approximated as spheres, each with random sizes, filling a cube (represent- ing the hypothetical rock sample) in a random distribution. Utilizing a simple collision detection technique, a 3D model depicting these spheres filling the space can be obtained. This 3D model has then been sliced into 2D images to generate both low and high-resolution images. Figure 4 shows a sample cube (rock sample) and one of the 2D slices. This technique is capable of rapidly generating abundant data within a short time frame. While the produced images could potentially be in color and closely resemble real tomography samples, we have applied a binary filter to them (see Figure 5). Following this filtering process, white re- gions correspond to rock, while black regions represent the pores. This simplification enhances the images, streamlining the training process for the model.

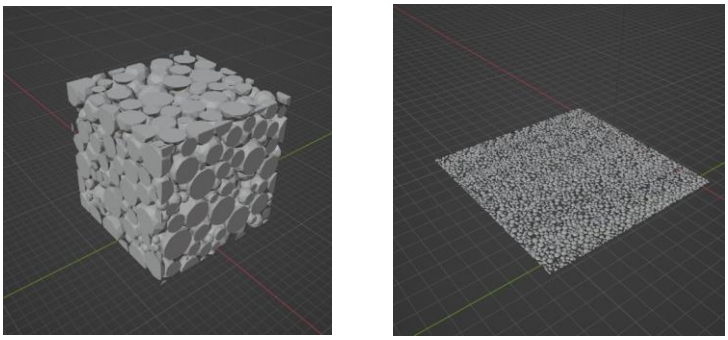

Figure 4- Rock model (left) and rock slices made on Blender (right)

Source: Made by the authors

Figure 5- Raw synthetic data (left) and binarized synthetic data (right)

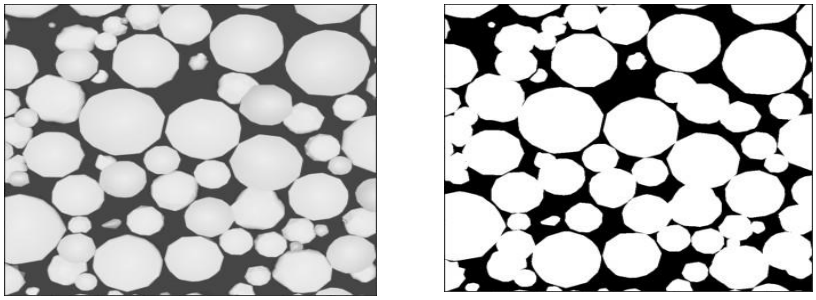

Source: Made by the authors

3.3 Transfer learning

Transfer Learning is a machine learning technique where a model trained on one task is re-purposed for another related task. A pre-trained model transfers the knowledge gleaned from a larger synthetic dataset to the primary neural network. This network then performs the main inference on the real images. By utilizing the base model, trained on the synthesized data, SRCNN gains access to a broader spectrum of examples for training. This transfer of knowledge enables SRCNN to learn relevant features from the base model, alleviating the need for extensive real data collection and enhancing the model ability to generalize even with a smaller dataset.

3.4 Base model training with synthetic data

The model based on the SRCNN architecture has been trained using 512 synthetic images. As depicted in Figure 7 and Table 2, the model demonstrates exceptional performance on synthetic data, which is notably simpler. However, it is important to note that this high level of performance may not translate as effectively to real-world data due to its increased complexity and variability of the real world data.

Figure 7- Low-resolution image (left), model response (middle), high-resolution image (right)

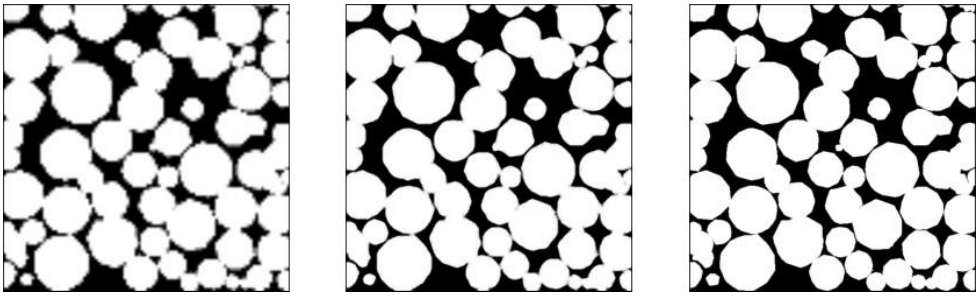

Source: Made by the authors.

Table 2- Comparative analysis of LR image and Model response against HR image

	SSIM	MSE
LR image vs. HR image	0.7780	0.0183
Model response vs. HR image	0.8860	0.0103

Source: Made by the authors.

3.5 Full model training with transfer learning

The model based on the SRCNN architecture has been trained on the DRSRD1-2D dataset. However, the training was started from the weights obtained from the base model (trained on the synthetic images), rather than random initial weights as previously outlined in this section. The outcomes are illustrated in Figure 8 and Table 3, where the model performance after being trained with 512 samples of real sandstone images is depicted. As evident from the results, the model effectively enhances the resolution of LR images.

Table 3- Comparative analysis of LR image and Full Model response against HR image

	SSIM	MSE
LR image vs. HR image	0.4798	0.0079
Full Model response vs. HR image	0.5197	0.0069

Source: Made by the authors.

Figure 8- Low-resolution image (left), Full Model response (middle), high-resolution image (right)

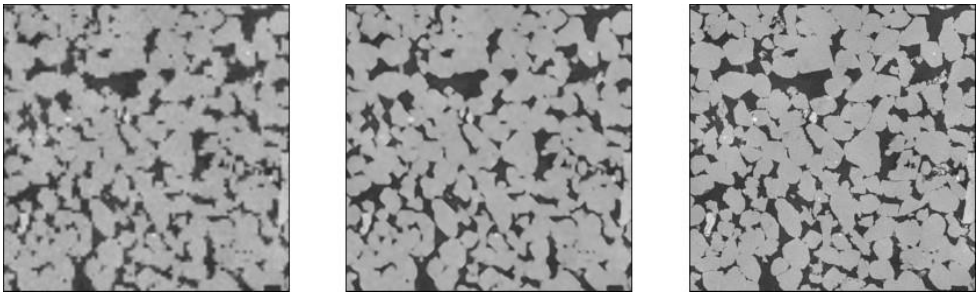

Source: Made by the authors.

4 Results

In this section, we provide a detailed comparison between a pure SRCNN model and a SRCNN allied with transfer learning. Our objective is to thoroughly analyze their performance across different experimental conditions and dataset sizes. The model was trained with and without transfer learning on varying sizes datasets containing 64, 128, 256 and 512 images from the DRSRD1-2D dataset so we could compare the performances for different dataset sizes. Henceforth, in accordance with the terminology adopted in this study, the model trained using transfer learning will be referred to as TL-SRCNN.

The following graphs display the validation loss curves during training, for each of the dataset sizes, and comparing the models with and without the transfer learning step. The graphs depicted in Figure 9 illustrate a comparison of validation loss trends throughout the training process across various dataset sizes. Notably, TL-SRCNN consistently demonstrates superior performance compared to the base model SRCNN across all dataset sizes. However, It is noticeable that the magnitude of performance disparity between TL- SRCNN and SRCNN diminishes as the dataset size increases. In other words, while TL-SRCNN maintains its advantage over SRCNN across different dataset scales, the extent of this advantage gradually decreases with using larger datasets. This is mainly due to the fact that a bigger (real) dataset has enough information to learn all the most important features of the mapping between low-resolution and high-resolution images. Figure 10 compares model performance for different settings. The graph for TL-SRCNN shows a significant decrease in validation loss between 64 and 128 images, but a smaller difference between 256 and 512 images, confirming that these larger datasets are enough for the model to learn the most important features.This result demonstrates that TL-SRCNN has a visible improvement in performance when dataset size is limited. To provide a comprehensive comparison of model performance, Table 4 presents the average SSIM and MSE metrics calculated across all images in the dataset. As anticipated from the validation loss results, TL-SRCNN consistently outperforms base SRCNN in both metrics, particularly evident in smaller datasets. These results further underscore the efficacy of transfer learning techniques, especially in scenarios with constrained dataset sizes. Finally, Figures 11a and 11b, accompanied by Table 5, showcase a sample from the dataset through TL-SRCNN and SRCNN models trained with dataset sizes of 64 and 256. Notably, TL-SRCNN consis- tently outperforms the standard SRCNN, as evidenced by the results depicting the SSIM and MSE values in comparison to the HR image.

Table 4- Comparative analysis of TL-SRCNN and SRCNN performance across varying Dataset sizes

	TL-SRCNN		SRCNN	
Dataset size	SSIM	MSE	SSIM	MSE
64	0.5031	0.0069	0.4815	0.0075
128	0.5090	0.0068	0.4963	0.0071
256	0.5111	0.0067	0.4901	0.0073

512	0.5152	0.0066	0.5125	0.0067

Source: Made by the authors.

Figure 9- Comparison of Validation Loss between TL-SRCNN and SRCNN across different Dataset sizes

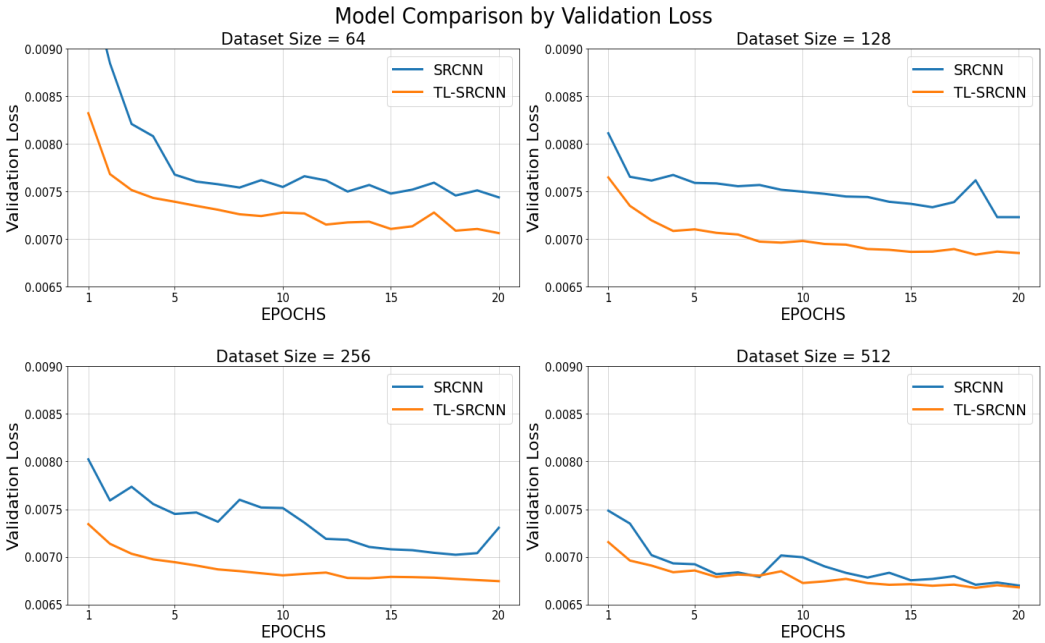

Source: Made by the authors.

Table 5- Comparative analysis of TL-SRCNN and SRCNN against target HR image

	Dataset size 64		Dataset size 256	
	SSIM	MSE	SSIM	MSE
SRCNN Output vs. target HR image	0.4809	0.0076	0.4961	0.0074
TL-SRCNN Output vs. target HR image	0.5038	0.0070	0.5201	0.0068

Source: Made by the authors.

Figure 10- Validation Loss for TL-SRCNN (left) and SRCNN (right) across different Dataset sizes

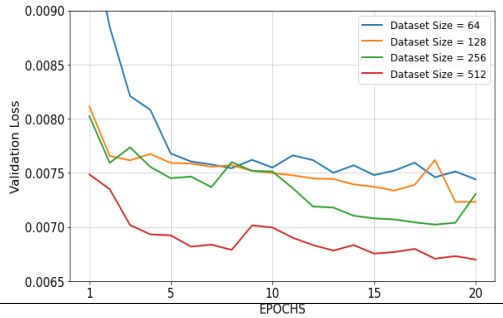

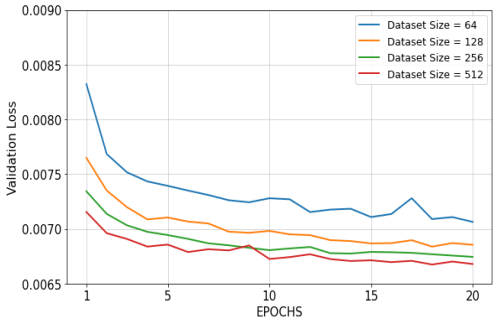

Source: Made by the authors.

Figure 11- Comparison of SRCNN and TL-SRCNN outputs against target HR image with different Dataset sizes

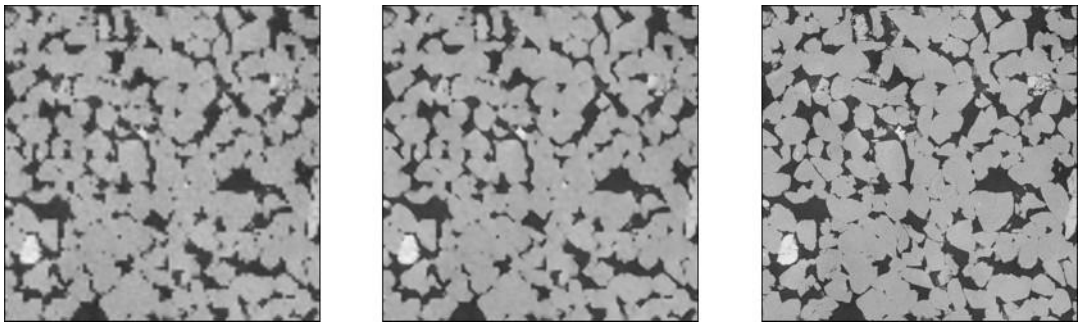

(a) Dataset size 64: SRCNN output (left), TL-SRCNN output (middle) and target HR image (right)

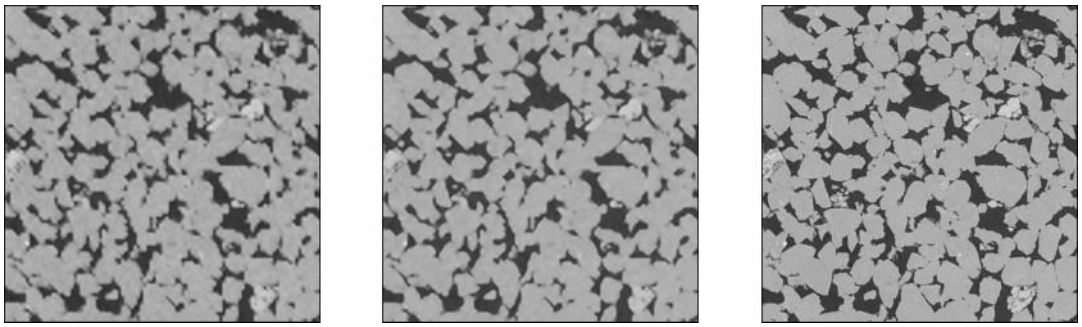

(b) Dataset size 256: SRCNN output (left), TL-SRCNN output (middle) and target HR image (right)

Source: Made by the authors.

5 Conclusion

An approach was proposed to address the challenge of extensive real data collection, which incurs significant costs in the oil and gas industry. Synthetic data was generated and used to pre-train a model, which was subsequently fine-tuned with a smaller dataset of real sandstone images. This approach yielded noticeable performance improvements and reduced the reliance on large

datasets. Evaluation using SSIM and MSE metrics indicated that TL-SRCNN outperforms standard SRCNN, even with smaller datasets, as intended. These results suggest that the integration of transfer learning with SRCNN presents a promising solution for obtaining high-quality underground images while addressing computational, instrumental, and financial constraints. The synthetic data utilized in this study was generated solely using spheres. However, in future endeavors, incorporating more realistic models of various grains could introduce additional physics into the synthetic dataset, potentially enhancing the overall performance of the TL-SRCNN model.

Referências

Ahuja, V. R., Gupta, U., Rapole, S. R., Saxena, N., Hofmann, R, Day-Stirrat, R. J., & Yalavarthy, P. K. (2022). Siamese-SR: A Siamese Super-Resolution Model for Boosting Resolution of Digital Rock Images for Improved Petrophysical Property Estimation. IEEE Transactions on Image Processing, 31, 3479–3493. https://doi.org/DOI: 10.1109/TIP.2022.3172211

Blöcher, G., & Zimmermann, G. (2008). Settle3D—A numerical generator for artificial porous media. Computers & Geosciences, 34(12), 1827–1842. https://doi.org/10.1016/j.cageo.2007.12.008

Cai, Z., Yang, Y., Meng, J., Qiu, S., Lei, L., & Xu, P. (2024). Resolution enhancement and deblurring of porous media μ-CT images based on super resolution generative adversarial network. Geoenergy Science and Engineering, 236, 212753. https://doi.org/10.1016/j.geoen.2024.212753

Da Wang, Y., Mostaghimi, P., & Armstrong, R. (2019). A super resolution dataset of digital rocks (drsrd1): Sandstone and carbonate. Digital Rocks Portal. https://doi.org/DOI:10.17612/P7D38H

Da Wang, Y., Shabaninejad, M., Armstrong, R. T., & Mostaghimi, P. (2021). Deep neural networks for improving physical accuracy of 2D and 3D multi-mineral segmentation of rock micro-CT images. Applied Soft Computing, 104, 107185. https://doi.org/10.1016/j.asoc.2021.107185

Dong, C., Loy, C. C., He, K., & Tang, X. (2015). Image super-resolution using deep convolutional networks. IEEE Transactions on Pattern Analysis and Machine Intelligence, 38(2), 295–307. https://doi.org/10.1109/TPAMI.2015.2439281

Karimpouli, S., Kadyrov, R., Siegert, M., & Saenger, E. H. (2023). Applicability of 2D algorithms for 3D characterization in digital rocks physics: an example of a machine learning-based super resolution image generation. Applied Geophysics, 1–14. https://doi.org/10.1007/s11600-023-01149-7

Ledig, C., Theis, L., Huszár, F., Caballero, J., Cunningham, A., Acosta, A., Aitken, A., Tejani, A., & et al. (2017). Photo-realistic single image super-resolution using a generative adversarial network. In Proceedings of the IEEE Conference on Computer Vision and Pattern Recognition, 4681--4690. https://doi.org/10.1109/CVPR.2017.51

Lim, B., Son, S., Kim, H., Nah, S., & Mu Lee, K. (2017). Enhanced deep residual networks for single image super-resolution. In Proceedings of the IEEE Conference on Computer Vision and Pattern Recognition Workshops, 136–144. https://doi.org/10.1109/CVPRW.2017.24

Luo, X., Sun, J., Zhang, R., Chi, P., & Cui, R. (2024). A multi-condition denoising diffusion probabilistic model controls the reconstruction of 3D digital rocks. Computers & Geosciences, 184, 105541. https://doi.org/10.1016/j.cageo.2024.105541

Park, S. C., Park, M. K., & Kang, M. G. (2003). Super-resolution image reconstruction: a technical overview. IEEE Signal Processing Magazine, 20(3), 21-36. https://doi.org/10.1109/MSP.2003.1203207

Soltanmohammadi, R., & Faroughi, S. A. (2023). A comparative analysis of super-resolution techniques for enhancing micro-CT images of carbonate rocks. Applied Computing and Geosciences, 20, 100143. https://doi.org/10.1016/j.acags.2023.100143

Wang, Y., Teng, Q., He, X., Feng, J., & Zhang, T. (2019). CT-image of rock samples super resolution using 3D convolutional neural network. Computers & Geosciences, 133, 104314. https://doi.org/10.1016/j.cageo.2019.104314

Wang, Z., Bovik, A. C., Sheikh, H. R., & Simoncelli, E. P. (2004). Image quality assessment: from error visibility to structural similarity. IEEE Transactions on Image Processing, 13(4), 600–612. https://doi.org/10.1109/TIP.2003.819861

Yang, D., & Jiabao, B. (2021). An optimization method for video upsampling and downsampling using interpolation-dependent image downsampling. 2021 4th International Conference on Information Communication and Signal Processing (ICICSP), 438–442. https://doi.org/10.1109/ICICSP54369.2021.9611899

Zhang, Y., Li, K., Li, K., Wang, L., Zhong, B., & Fu, Y. (2018). Image super-resolution using very deep residual channel attention networks. Image Super-Resolution UsingIn Proceedings of the European Conference on Computer Vision (ECCV), 286–301. https://doi.org/10.48550/arXiv.1807.02758

Zhao, B., Saxena, N., Hofmann, R., Pradhan, C., & Hows, A. (2022). Enhancing resolution of micro-CT images of reservoir rocks using super resolution. Computers & Geosciences, 170, 105265. https://doi.org/10.1016/j.cageo.2022.105265

Access all Papers
biblioteca.ibp.org.br